

Supporting Information for

Organic Contaminant Release from Melting Snow:

I. Influence of Chemical Partitioning

TORSTEN MEYER,^{†,‡} YING DUAN LEI,^{†,‡} IBRAHIM MURADI,[‡] FRANK WANIA^{*,†,‡}

Department of Chemical Engineering and Applied Chemistry and Department of Physical and Environmental Sciences, University of Toronto at Scarborough, 1265 Military Trail, Toronto, Ontario, Canada, M1C 1A4

Content

Material		Page
Table S1	Physical-chemical properties of organic target substances	S2
Text	Calculations of the partition coefficients	S3
Table S2	Solute descriptors and enthalpies used in the calculations	S4
Text	Comparison with the results from Schöndorf and Herrmann (1987)	S5
Figure S1	Relative elution sequences of organic chemicals from Schöndorf and Herrmann (1987) and from this study.	S6
Figure S2	$\log (K_{IA}/m)$ value vs. percentage loss during dry and wet snow metamorphism for five target substances.	S7
Figure S3	Relative dielectric permittivity reflecting melt water content and dry snow density vs. time for different snow depths; describes the early melt phase in the applied melt scenario.	S8
Figure S4	Indicator value R that quantifies the fraction of the chemical which is present in the liquid melt water phase of the snow pack.	S9
Text	References	S10

Table S1 Physical-chemical properties at 0 °C of the organic contaminants used in this study.

	solubility in water ($\mu\text{g/L}$)^b	log (K_{IA}/m)	log $K_{\text{HA/W}}$	log K_{AW}	log (K_{IW}/m)
Atrazine	15,000	1.5	2.4	-7.3	-6.3
Naphthalene	13,700	-3.2	3.2	-2.5	-5.7
Lindane	2,500	-0.2	3.5	-4.8	-5.0
Phenanthrene	390	-1.4	4.5	-3.2	-4.6
Pyrene	49	-0.2	4.9	-3.8	-4.0
Fluoranthene ^a	0.26	-0.8	5.3	-4.3	-5.1
Benzo(ghi)perylene	0.049	2.1	6.6	-5.2	-3.1

^a fluoranthene was used by Schöndorf and Herrmann (1987)

^b from Mackay et al. (2006).

Calculation of the Partition Coefficients for Figure 1

Snow-air partition coefficient log (K_{IA}/m)

The poly-parameter linear free energy relationship (pp-LFER) for the calculation of the snow - air partition coefficient was taken from Roth et al. (2004):

$$\log K_{IA} (-6.8\text{ }^{\circ}\text{C}) = 3.53 \sum \alpha_2^H + 3.38 \sum \beta_2^H + 0.639 \log L^{16} - 6.85,$$

where $\log L^{16}$ is the hexadecane/air partition coefficient at 25 °C, $\sum \alpha_2^H$ is the electron acceptor; and $\sum \beta_2^H$ is the electron donor of the particular substance. The solute descriptors are shown in Table S2. The $\log K_{IA}$ values were temperature corrected using:

$$\log K_{IA} (T) = \log K_{IA} (T_{ref}) + \frac{\Delta H_{IA}}{2.303 R} \left[\frac{1}{T_{ref}} - \frac{1}{T} \right]$$

where ΔH_{IA} is the enthalpy of sorption (Table S2).

Air-water partition coefficient log K_{AW}

The $\log K_{AW}$ value of lindane was calculated from a FAV by Xiao et al. (2004) and that of atrazine was taken from Mackay et al. (2006). The $\log K_{AW}$ values of the PAHs except pyrene were calculated from Henry's law constant expressions in Mackay et al. (2006) (van't Hoff eq. derived from literature data, Staudinger and Roberts, 2001). The $\log K_{AW}$ value of pyrene was calculated from a Henry's law constant expression in Mackay et al. (2006) (gas stripping-GC, Bamford et al., 1999).

Humic acid-water partition coefficient log [$K_{HA/W}/(L/kg)$]

The humic acid-water partition coefficients of all substances were calculated using the pp-LFER from Niederer et al. (2006): $\log [K_{HA/W}/(L/kg_{HA})] = 0.29 L + 2.50 V - 3.29 B - 0.21 A - 0.79 S + 0.01$. The solute descriptors are shown in Table S2.

Snow-water partition coefficient log ($K_{I/W}/m$)

The snow-water partition coefficient of all chemicals was calculated using the equation:

$$\log (K_{I/W}/m) = \log (K_{I/A}/m) + \log K_{AW}$$

Table S2 Solute descriptors and enthalpies used in the calculations.

Substance	A ($\sum \alpha_2^H$)	B ($\sum \beta_2^H$)	L ($\log L^{16}$)	V	S	ΔH_{IA} [kJ mol ⁻¹] ^g
Atrazine ^a	0.17	1.01	7.783	1.6196	1.29	-129.0
γ -HCH ^b	0.00	0.68	7.467	1.5798	0.91	-95.9
Naphthalene ^c	0.00	0.20	5.161	1.0854	0.92	-60.1
Phenanthrene ^c	0.00	0.26	7.63	1.454	1.29	-81.9
Pyrene ^c	0.00	0.29	8.83	1.585	1.71	-98.6
Fluoranthene	0.00 ^d	0.20 ^d	8.83 ^e	1.585 ^d	1.53 ^d	-60.1
Benzo(ghi)perylene	0.00 ^f	0.35 ^f	13.25 ^e	1.547 ^f	0.70 ^f	-122.7

^a from Abraham et al. (2007).

^b from Abraham et al. (2002).

^c from Goss (2005), Supplementary Data

^d from Poole and Poole (1999).

^e from Abraham (1993).

^f from Luehrs et al. (1996).

^g calculated from eq. 8 in Lei and Wania (2004) based on the pp-LFER by Roth et al. (2002) and an empirical relationship by Goss and Schwarzenbach (1999).

Comparison with the Results from the Study by Schöndorf and Herrmann (1987).

In the only other published laboratory study that investigated the fractionated release of organic contaminants in melting snow (Schöndorf and Herrmann, 1987), the observed elution patterns closely resemble those reported here (Fig. S1). PYR and fluoranthene (FLT) have similar partition coefficients (Table S1), hence, their snowmelt behavior should not differ very much. Although Schöndorf and Herrmann (1987) did not distinguish between dissolved and particulate phases, we may infer that the two concentration peaks of LIN at the beginning and at the end of the melt period refer to the dissolved and the particulate fraction, respectively (Fig. S1). Their study shows a stronger amplification of LIN within the first melt water sample compared to this study. The snow column Schöndorf and Herrmann used in their experiments promotes such a first chemical flush. A snow pack with a depth of 100 cm contains a larger fraction of LIN that is concentrated at the snow grain surfaces and that can be taken up by the first melt water. Furthermore, the small horizontal area of 154 cm² such as used in their study prevents the development of distinct flow fingers that could flatten this concentration peak. In both studies the bulk of the more hydrophobic substances FLT, PYR, and BghiP was retained in the snow pack until the very end of the melt period while attached to the particles. The concentration ratios of the three substances provide hints on how the partitioning properties affect the melt behavior (Fig. S1). Both ratios FLT/LIN and PYR/LIN increase in the second half of the melt period reflecting the higher water solubility of LIN. The latter was washed out in notable concentrations over the entire melt period. The release of FLT and PYR, on the other hand is characterized by a stronger Type 2 enrichment. The ratios of FLT and PYR, respectively, to BghiP are very similar in both studies. At the beginning of the melt period a slightly enhanced particle load is washed out until an increasing snow density and stronger particle coagulation hamper a further release of particles. Both FLT and PYR are more water soluble than BghiP. Accordingly, their concentrations in relation to BghiP increase until a peak is reached. The subsequently decreasing ratios may be explained by decreasing amounts of FLT and PYR at the snow grain surfaces, that are available to become dissolved in the aqueous melt water phase. Furthermore, the transfer of FLT or PYR from the particulate into the dissolved phase decreases because parts of those substances are

more strongly bound due to the formation of chemical bonds or by inclusion into coagulates (Schöndorf and Herrmann, (1987).

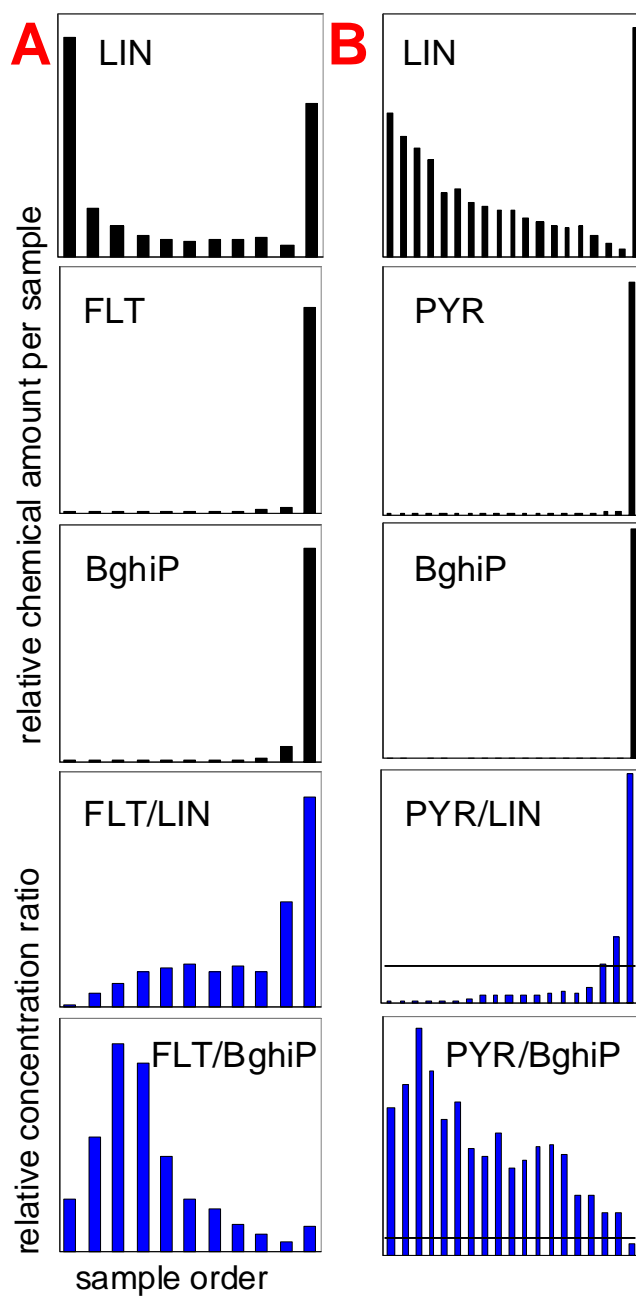


Figure S1 Relative elution sequences of lindane (LIN), fluoranthene (FLT), pyrene (PYR) and benzo-ghi-perylene (BghiP) reported in (Schöndorf and Herrmann, 1987) (A) compared with those of this study (B). The horizontal line refers to the concentration ratio of 1. The particulate and dissolved fractions of this study were combined.

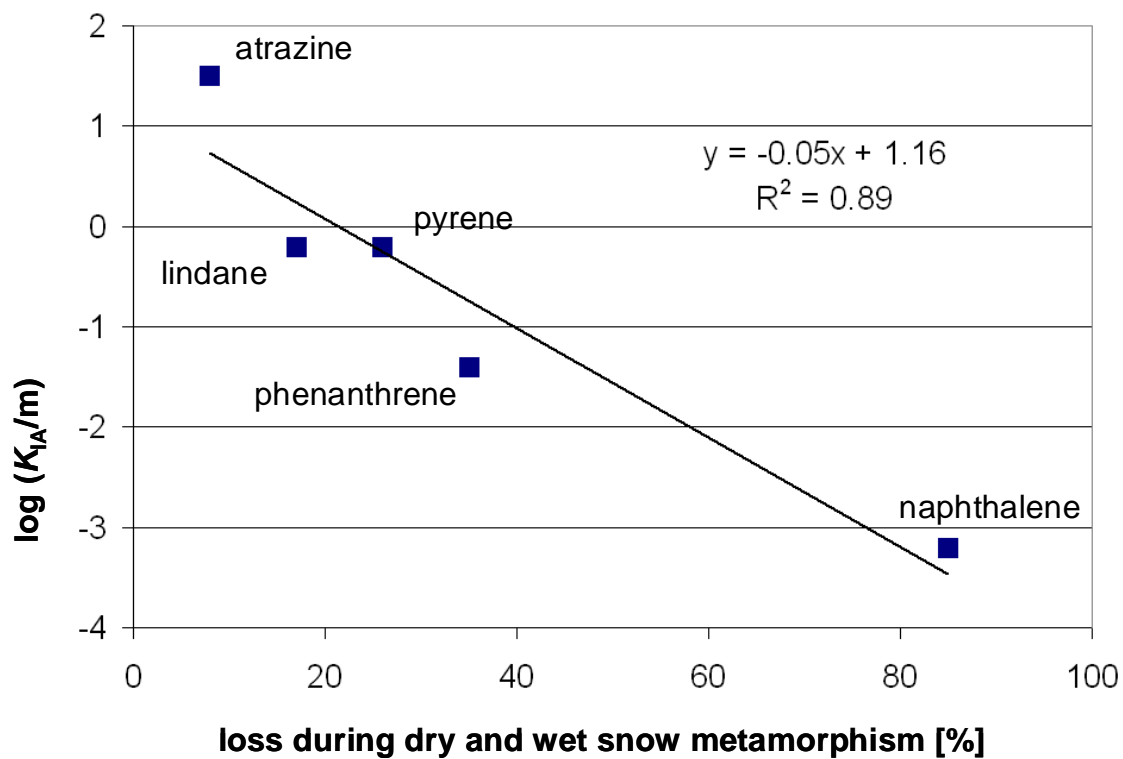


Figure S2 regression of $\log(K_{IA}/m)$ vs. percentage evaporation loss during dry and wet snow metamorphism for five target chemicals.

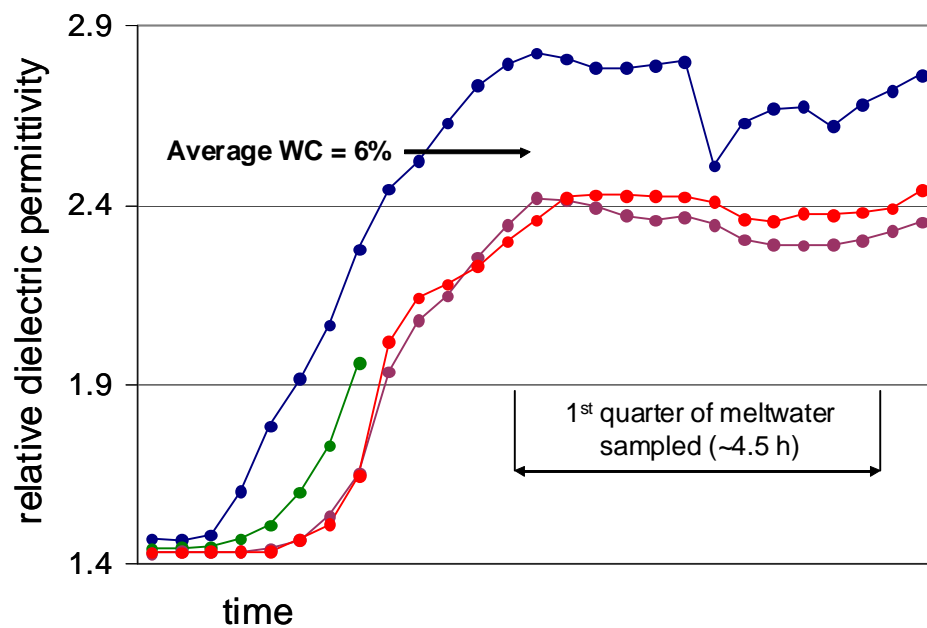


Figure S3 Relative dielectric permittivity reflecting melt water content and dry snow density vs. time for different snow depths; describes the early melt phase in the applied melt scenario (scenario B in Meyer et al., this issue).

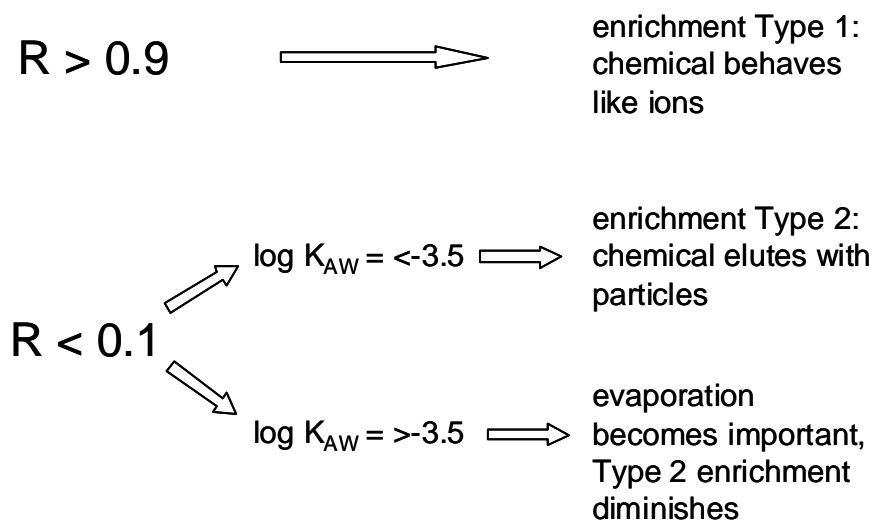


Figure S4 R-value that quantifies the fraction of the chemical which is present in the liquid melt water phase of the snow pack, and indicates Type 1 and Type 2 chemical enrichment.

References

- Abraham, M.H. Hydrogen bonding XXVII. Solvation parameters for functionally substituted aromatic compounds and heterocyclic compounds, from gas-liquid chromatographic data. *J. Chromatogr.* **1993**, 644, 95-139.
- Abraham, M.H., Enomoto, K., Clarke, E.D., Sexton, G. Hydrogen bond basicity of the chlorogroup; hexachlorocyclohexanes as strong hydrogen bond bases. *J. Org. Chem.* **2002**, 67, 4782-4786.
- Abraham, M.H., Enomoto, K., Clarke, E.D., Rosés, M., Ràfols, C., Fuguet, E. Henry's law constants or air to water partition coefficients for 1,3,5-triazines by an LFER method. *J. Environ. Monitor.* **2007**, 9, 234-239.
- Bamford, H.A., Poster, D.L., Baker, J.E. Temperature dependence of Henry's law constants of thirteen polycyclic aromatic hydrocarbons between 4°C and 31°C. *Environ. Toxicol. Chem.* **1999**, 18, 1905-1912.
- Goss, K.-U.; Schwarzenbach, R.P. Empirical prediction of heats of vaporization and heats of adsorption of organic compounds. *Environ. Sci. Technol.* **1999**, 33, 3390-3393.
- Goss, K.-U. Predicting the equilibrium partitioning of organic compounds using just one linear solvation energy relationship (LSER). *Fluid Phase Equilibria* **2005**, 233, 19-22.
- Lei, Y.D.; Wania, F. Is rain or snow a more efficient scavenger of organic chemicals? *Atmos. Environ.* **2004**, 38, 3557-3571.
- Luehrs, D.C., Hickey, J.P., Nilsen, P.E., Godbole, K.A., Rogers, T.N. Linear solvation energy relationship of the limiting partition coefficient of organic solutes between water and activated carbon. *Environ. Sci. Technol.* **1996**, 30, 143-152.
- Mackay, D., Shiu, W.Y., Ma, K.-C., Lee, S.C. (2006) Physical-chemical properties and environmental fate for organic chemicals. Handbook-Second Edition, CRC Press, Taylor & Francis, Boca Raton, FL.
- Meyer, T., Lei, Y.D., Wania, F., Muradi, I. Organic contaminant release from melting snow: II. Influence of snow pack and melt characteristics. *Environ. Sci. Technol.*, this issue.

Niederer, C., Goss, K.-U., Schwarzenbach, R.P. Sorption equilibrium of a wide spectrum of organic vapors in Leonardite humic acid: modeling of experimental data. *Environ. Sci. Technol.* **2006**, *40*, 5374-5379.

Poole, S.K., Poole, C.F. Chromatographic models for the sorption of neutral organic compounds by soil from water and air. *J. Chromatogr. A* **1999**, *845*, 381-400.

Roth, C.M., Goss, K.-U., Schwarzenbach, R.P. Adsorption of a diverse set of organic vapors on the bulk water surface. *J. Colloid Interf Sci.* **2002**, *252*, 21-30.

Roth, C.M., Goss, K.-U., Schwarzenbach, R.P. Sorption of diverse organic vapors to snow. *Environ. Sci. Technol.* **2004**, *38*, 4078-4084.

Schöndorf, T.; Herrmann, R. Transport and chemodynamics of organic micropollutants and ions during snowmelt. *Nordic Hydrology* **1987**, *18*, 259-278.

Staudinger, J., Roberts, P.V. A critical compilation of Henry's law constant temperature dependence relations for organic compounds in dilute aqueous solutions. *Chemosphere* **2001**, *44*, 561-576.

Xiao, H., Li, N., Wania, F. Compilation, evaluation and selection of physical-chemical properties for α -, β -, and γ -hexachlorocyclohexane. *J. Chem. Eng. Data* **2004**, *49*, 173-185